

1       **A parsimonious regional parametric evapotranspiration**  
2       **model based on a simplification of the Penman-Monteith**  
3                               **formula**

4  
5       A. Tegos<sup>1\*</sup>, N. Malamos<sup>2</sup> and D. Koutsoyiannis<sup>1</sup>

6  
7       <sup>1</sup>*Department of Water Resources and Environmental Engineering, National Technical*  
8       *University of Athens, Heroon Polytechniou 5, GR-157 80, Zographou, Greece*

9       <sup>2</sup>*Department of Agricultural Technology, Technological Educational Institute of Western Greece,*  
10       *Amaliada, Greece*

11       [\\*tegosaris@yahoo.gr](mailto:*tegosaris@yahoo.gr)

12  
13       **Abstract** Evapotranspiration is a key hydrometeorological process and its estimation is important in  
14       many fields of hydrological and agricultural sciences. Simplified estimation proves very useful in  
15       absence of a complete data set. In this respect, a parametric model based on simplification of the  
16       Penman-Monteith formulation is presented. The basic idea of the parametric model is the  
17       replacement of some of the variables and constants that are used in the standard Penman-Monteith  
18       model by regionally varying parameters, which are estimated through calibration. The model is  
19       implemented in various climates on monthly time step (USA, Germany, Spain) and compared on  
20       the same basis with four radiation-based methods (Jensen-Haise, McGuinness and Bordne,  
21       Hargreaves and Oudin) and two temperature-based (Thornthwaite and Blaney-Criddle). The  
22       methodology yields very good results with high efficiency indexes, outperforming the other models.  
23       Finally, a spatial analysis including the correlation of parameters with latitude and elevation  
24       together with their regionalization through three common spatial interpolation techniques along  
25       with a recent approach (Bilinear Surface Smoothing), is performed. Also, the model is validated  
26       against Penman-Monteith estimates in eleven stations of the well-known CIMIS network. The total  
27       framework which includes the development, the implementation, the comparison and the mapping

28 of parameters illustrates a new parsimonious and high efficiency methodology in the assessment of  
29 potential evapotranspiration field.

30 **Key words:** Potential evapotranspiration, Penman- Monteith method, Parametric model,  
31 Calibration, Spatial analysis  
32

33

## 34 1. Introduction

35 Accurate estimation of evapotranspiration has gained scientific interest due to high  
36 importance in hydrological modelling, irrigation planning and water resources  
37 management. According to Farquhar and Roderick (2007), changes in evaporative  
38 demand affect fresh water supplies and have impact on agriculture, the biggest  
39 consumer of fresh water. Estimating water requirements for irrigation purposes goes  
40 back to 1890 in the USA (Jensen and Haise, 1963).

41 The vast number of scientific attempts to estimate Potential Evapotranspiration  
42 (PET) or Reference Evapotranspiration (ET<sub>o</sub>) depicts the significant role of  
43 evapotranspiration in irrigation water management Those attempts yielded about 50  
44 evapotranspiration models (Lu *et al.* 2005, McMahon *et al.* 2013) which can be  
45 grouped into seven classes: (i) empirical, (ii) water budget (iii) energy budget, (iv)  
46 mass transfer, (v) combination, (vi) radiation and (vii) measurement (Xu and Singh  
47 2000).

48 The plethora of models and frameworks arises from the complexity of the  
49 physical phenomenon, the availability of the necessary hydrometeorological data and  
50 the variability of local climatic conditions.

51 The Penman-Monteith formulation (Monteith 1981) was proposed by FAO as  
52 the standard method for computing Potential Evapotranspiration (PET) (Allen *et al.*  
53 1989) and has had numerous successful applications in hydrology and  
54 agrometeorology in various hydroclimatic regimes (Wang and Georgakakos 2007).

55 Basic drawback of the model's applicability is the requirement of several climatic  
56 data like temperature, wind speed, relative humidity and radiation. Such  
57 measurements are not always easily available or accessible to researchers due to the  
58 sparse hydrometeorological stations networks in several regions, e.g. Africa, as well  
59 as the instability in the records of radiation and relative humidity (Samani, 2000).  
60 Therefore, the demand of new simplified models in several time scales (Alexandris  
61 and Kerkides 2003, Oudin *et al.* 2005, Valiantzas, 2013,) like radiation-based and  
62 temperature-based models, is justified. Several publications (Tabari 2010, Samaras *et*  
63 *al.* 2014) demonstrated that radiation-based methods are capable for PET estimation.  
64 Additionally, many researchers suggest the need for further model calibration  
65 (especially in the energy term of radiation) to improve the overall efficiency (Irmak *et*  
66 *al.* 2003, Zhai L. *et al.* 2010, Azhar and Perera 2010, Thepadia and Martinez 2012,  
67 Tabari and Talalee 2011).

68 This study presents a radiation-based model that introduces an innovative  
69 approach in the estimation of potential evapotranspiration. This methodology that  
70 requires only temperature data incorporates a new concept concerning local  
71 calibration needs and produces a parsimonious expression for the potential  
72 evapotranspiration estimation by replacing some of the variables and constants that  
73 are used in the standard Penman-Monteith model by regionally varying parameters,  
74 which are estimated through calibration. The model is implemented and compared to  
75 established radiation and temperature based methods using the available data from 53  
76 hydrometeorological stations of USA, Germany and Spain, representing different  
77 climate conditions, both arid and humid. Finally, analyses concerning: (a) the  
78 parameters' dependence on latitude and (b) the parameters' spatial variability, was  
79 performed based on data from the California Irrigation Management Information

80 System (CIMIS - Hart *et al.* 2009) programme that was introduced by the California  
81 Department of Water Resource and the University of California, Davis, in 1982. For  
82 the latter, the calibration procedure incorporates 39 CIMIS stations, while the  
83 validation is made against the calculated parameter values from a set of 11 additional  
84 stations.

85

## 86 **2. Materials and methods**

### 87 **2.1 Penman-Monteith model and radiation-based methods**

88 The classic model of the Penman-Monteith (Monteith 1965) equation to estimate  
89 potential evaporation or evapotranspiration is expressed as:

$$90 \text{ PET} = \frac{\Delta}{\Delta + \gamma'} \frac{R_n}{\lambda} + \frac{\gamma}{\Delta + \gamma'} F(u) D, \gamma' = \gamma (1 + r_s/r_a) \quad (1)$$

91 where PET is potential evaporation or evapotranspiration (mm/d),  $R_n$  is net radiation  
92 at the surface  $\Delta$  is the slope of the saturation vapor pressure curve,  $\gamma$  is psychometric  
93 coefficient while  $r_s$  and  $r_a$  are the surface and aerodynamic resistance factors.

94 Jensen and Haise (1963) evaluated 3000 observations of ET as determined by  
95 soil sampling procedures over a 35-year period, and developed an equation that  
96 requires only the average daily temperature and the extraterrestrial radiation, while  
97 one decade later, McGuinness and Bordne (1972) using lysimeter data suggested a  
98 slight modification to Jensen's formulation.

99 Another widely used approach is the Hargreaves model (Hargreaves and  
100 Samani 1982) that estimates the reference evapotranspiration at monthly and daily  
101 scale. The method has received considerable attention because it can produce very  
102 acceptable results under diverse climates using only temperature and radiation  
103 measurements (Shahidian *et al.* 2013). According to several researchers (Samani

104 2000, Xu and Singh 2002) the method performs poorly in extreme humidity and wind  
105 conditions.

106 A recent study (Oudin *et al.* 2005), evaluated a number of evapotranspiration  
107 methods, on the basis of precipitation and streamflow data from a large sample of  
108 catchments in the USA, France and Australia. After extended analysis with the use of  
109 four hydrological models, the researchers modified the Jensen and McGuinness model  
110 and proposed a generalized radiation- based equation.

111 Table 1 summarizes the expressions that estimate PET according to the above-  
112 mentioned methodologies:

113 **Table 1**

114 where PET ( $\text{mm d}^{-1}$ , equivalent to  $\text{kg m}^{-2} \text{d}^{-1}$  of the dimensionally consistent Penman-  
115 Monteith equations) is the potential evapotranspiration,  $R_a$  ( $\text{kJ m}^{-2}\text{d}^{-1}$ ) is the  
116 extraterrestrial shortwave radiation,  $T_a$  ( $^{\circ}\text{C}$ ) is the air temperature,  $\lambda$  is the latent heat  
117 of vaporization ( $\text{kJ kg}^{-1}$ ) and  $\rho$  is the water density ( $\text{kg L}^{-1}$ ).

118  
119 **2.2 Temperature-based methods**

120 The Thornthwaite model (Thornthwaite, 1948) is the most simplified method and  
121 requires only temperature measurements. The model's form is:

122 
$$\text{PET} = 1.6 L_d \left( \frac{10 T_a}{I} \right)^a \quad (2)$$

123 where PET is the potential evapotranspiration (mm/month),  $L_d$  is the daytime length,  
124  $T_a$  is the mean monthly air temperature ( $^{\circ}\text{C}$ ),  $I$  is the annual heat index and  $a$  is an  
125 empirically determined parameter which is function of  $I$ .

126 The Blaney-Criddle method (Blaney and Criddle, 1962) has received  
127 worldwide application for the estimation of irrigation demands. The model expression  
128 is:

129  $PET = K p (0.46 T_a + 8.13)$  (3)

130 where PET is the potential evapotranspiration (mm/month),  $T_a$  the mean temperature  
131 ( $^{\circ}\text{C}$ ),  $K$  is the monthly consumptive use coefficient and  $p$  is the mean daily percentage  
132 of annual daytime hours.

133

### 134 **2.3 The parametric formula**

135 The need of parsimonious model structure is essential in several fields of water  
136 resources sciences (Koutsoyiannis 2009, Koutsoyiannis 2014). This refers both to the  
137 model structure and to the input data, which should be easily available. Most of  
138 simplified formulas fail to describe the phenomenon of evapotranspiration due to its  
139 high complexity and the varying local climate conditions. Thus, the idea of replacing  
140 some variables and constants used in the standard Penman-Monteith (PM) formula by  
141 a number of parameters which are regionally varying and estimated through  
142 calibration from a reference evapotranspiration sample, constitutes a new appealing  
143 strategy for evapotranspiration estimation.

144 Koutsoyiannis and Xanthopoulos (1999), Tegos *et al.* (2009) and Tegos *et al.*  
145 (2013) examined the structure and the sensitivity of input data in PM model. They  
146 concluded that extraterrestrial radiation and temperature dominate in determining  
147 potential evapotranspiration. Furthermore, Mamassis *et al.* (2014) reached to the  
148 conclusion that the influence of every meteorological parameter in evaporation is  
149 almost linear, with temperature having the greater influence.

150 By dividing both the numerator and the denominator by  $\Delta$ , the PM equation  
151 can be written in the form:

152  $PET = \frac{1}{\lambda \rho} \frac{R_n + \gamma \lambda F(u) D}{1 + \gamma' / \Delta}$  (4)

153 In the above expression, the numerator is the sum of a term related to solar  
154 radiation and a term related to the rest of meteorological variables, while the  
155 denominator is function of temperature.

156 Based on the previous analysis, a simplification of the Penman-Monteith  
157 formula, where the numerator is approximated by a linear function of extraterrestrial  
158 solar radiation, while a linear descending function of temperature approximates the  
159 denominator, can be described by the following formula:

$$160 \text{ PET} = \frac{a R_a - b}{1 - c T_a} \quad (5)$$

161 where PET (mm) is the potential evapotranspiration,  $R_a$  ( $\text{kJ m}^{-2}$ ) is the extraterrestrial  
162 shortwave radiation calculated without measurements and  $T_a$  ( $^{\circ}\text{C}$ ) is the air  
163 temperature.

164 Equation (5) contains three parameters, i.e.  $a$  ( $\text{kg kJ}^{-1}$ ),  $b$  ( $\text{kg m}^{-2}$ ) and  $c$  ( $^{\circ}\text{C}^{-1}$ ),  
165 to which a physical interpretation can be assigned. Since extraterrestrial solar  
166 radiation is the upper bound of net shortwave radiation, the dimensionless term  
167  $a^* = a / \lambda \rho$  represents the average percentage of the energy provided by the sun (in  
168 terms of  $R_a$ ) and, after reaching the Earth's terrain, is transformed to latent heat, thus  
169 driving the evapotranspiration process. Parameter  $b$  lumps the missing information  
170 associated with aerodynamic processes, driven by the wind and the vapour deficit in  
171 the atmosphere. Finally, the expression  $1 - c T_a$  approximates the term:  $1 + \gamma / \Delta$ . We  
172 recall that  $\gamma'$  is a function of the surface and aerodynamic resistance (equation 1) and  
173  $\Delta$  is the slope vapour pressure curve, which is a function of  $T_a$ .

174

175 **2.4 Hydrometeorological data and computational tools**

176 For exploration purposes, we use monthly meteorological data from 39 CIMIS  
177 stations (Hart *et al.* 2009), available at [www.cimis.water.ca.gov](http://www.cimis.water.ca.gov), 10 stations from  
178 Germany and finally 4 stations from Spain (Table 2). The European data are freely  
179 available in the European Climate Assessment data set (Klok and Klein Tank, 2009 -  
180 <http://eca.knmi.nl/>). Stations' latitudes range from N 32.76° to N 53.38° and their  
181 altitude varies from 2.74 m to 1342.6 m.

182 The available data comprise mean temperature, relative humidity, sunshine  
183 duration and wind velocity. At all CIMIS stations the data covers the period from  
184 October 1992 to September 2012 while the European stations cover the period from  
185 January 1948 to December 2013. The choice of the time-periods was based on the  
186 simultaneous availability of the four required hydrometeorological variables  
187 (temperature, sunshine duration, humidity, wind speed). Additionally, the selection of  
188 each station and especially those from the CIMIS network was based on the existence  
189 of adequate length time series for the processes involved, i.e. 20 years.

190 **Table 2**

191 The time series processing along for the implementation of the different  
192 approaches for potential evapotranspiration estimation, i.e. Penman-Monteith,  
193 parametric and Hargreaves, was carried out using the free software application  
194 Hydrognomon (Kozanis *et al.* 2010, <http://hydrognomon.org/>), while the remaining  
195 expressions (Jensen, McGuinness and Oudin) were evaluated through spreadsheets.

196



197 2.5 **Statistical criteria**

198 The main statistical criterion used for the evaluation of the methodologies  
 199 performance against the values computed by the Penman Monteith method (PM) was  
 200 the coefficient of efficiency (CE), introduced by Nash & Sutcliffe (1970):

$$201 \quad CE = 1 - \frac{\sum_{i=1}^n (PE_i - PM_i)^2}{\sum_{i=1}^n (\overline{PM} - PM_i)^2} \quad (6)$$

202 where  $PM_i$  and  $PE_i$  are the potential evapotranspiration values of month  $i$ , computed  
 203 by the Penman-Monteith method and the other model respectively,  $\overline{PM}$  is the monthly  
 204 average over the common data period estimated by the Penman-Monteith formula  
 205 while  $n$  is the sample size.

206 Additionally, we applied several statistical measures, such as the mean bias error:

$$207 \quad MBE = \frac{1}{n} \sum_{i=1}^n (PE_i - PM_i) \quad (7)$$

208 the mean absolute error:  $MAE = \frac{1}{n} \sum_{i=1}^n |PE_i - PM_i|$  (8)

209 and the root mean square error:  $RMSE = \left[ \frac{1}{n} \sum_{i=1}^n (PE_i - PM_i)^2 \right]^{1/2}$  (9)

210 CE ranges between  $-\infty$  and 1 (1 inclusive), with  $CE = 1$  being the optimal  
 211 value. Values between 0 and 1 are generally regarded as acceptable levels of  
 212 performance, whereas values less than 0 indicate that the mean observed value is a  
 213 better predictor than the simulated value, which indicates unacceptable performance.

214 MBE, MAE and RMSE values of 0 indicate a perfect fit (Moriassi *et al.* 2007).

215

### 216 **3. Results**

217 The implementation of the parametric model was accomplished by calculating the  
218 three parameters involved at each station, as mentioned above. This procedure is  
219 automated via a least square optimization technique, embedded in the Hydrognomon  
220 software (Kozanis *et al.* 2010, <http://hydrognomon.org/>), providing means for  
221 acquiring optimized values of  $a$ ,  $b$  and  $c$  parameters for the parametric method  
222 application.

223 The calculated monthly Penman-Monteith potential evapotranspiration time  
224 series acted as the reference data sets against which the comparisons between the  
225 different methodologies took place. Table 3 summarizes the values of the parameters  
226 for each of the 53 stations, acquired by the procedure described above.

#### 227 **Table 3**

### 228 **3.1 Comparison with radiation-based methods**

229 Figure 1 presents the mean annual potential evapotranspiration calculated by the  
230 Penman-Monteith method for each one of the 39 CIMIS stations against the  
231 parametric and the other four methods. It is clear that the parametric, Hargreaves and  
232 McGuinness models respect the variation of the over-annual potential  
233 evapotranspiration, while the other two models, i.e. Oudin and Jensen-Haise  
234 underestimate and overestimate respectively, the potential evapotranspiration values.

#### 235 **Figure 1**

236 The performance indices presented in Table 4 confirm the good performance of the  
237 parametric method, which has the highest CE and excellent results in the other  
238 statistical indices. The Hargreaves model follows with CE 78.9%, similar MBE and  
239 worst MAE and RMSE than the parametric model. The McGuinness method gave

240 moderate results, while the Jensen-Haise and Oudin models totally fail to represent  
241 the physical flux.

242 **Table 4**

243 For further comparison of the parametric method against the four radiation-  
244 based methods, in terms of the achieved CE distribution from estimating monthly PE,  
245 each time series was split into two parts. The first 13 years were used as the  
246 calibration data set for the parametric model, while the remaining 7 years were used  
247 for validation. Table 5 presents the CE distribution, for the calibration (Cal) and the  
248 validation (Val) data set for 39 CIMIS stations, while that of the European stations is  
249 presented in Table 6.

250 **Table 5**

251 The results for both periods and in different climatic regimes are satisfactory  
252 for the parametric model, with the average CE values for the calibration period being  
253 94.80% for CIMIS stations and 96.52% for European stations, while for the validation  
254 period the corresponding values are 94.34% for CIMIS stations and 90.06% for the  
255 European stations. Altogether, the application of the parametric model in 26 stations  
256 from the 39 stations achieved CE values between 90 and 95%.

257 **Table 6**

258 The Hargreaves model achieved satisfactory results especially in the case of  
259 CIMIS network, where the model has been developed; while in European stations the  
260 acquired CE values are lower.

261 The McGuinness model acquired lower CE values in the CIMIS network than  
262 Parametric and Hargreaves with 87.14% in calibration period and 87.76% in the  
263 validation period. The Oudin model presented moderate results in the CIMIS network  
264 (52.18% in the calibration and 46.82% in the validation period) but considerably

265 better results in European stations (89.37 % calibration and 82.82% validation  
266 period). By taking into account the similar results presented by Tegos *et al.* (2013),  
267 the Oudin model seems to perform better in humid than in arid climatic conditions.

268 Finally, the Jensen-Haise model totally failed to produce physically  
269 meaningful results, since the achieved CE values were very low (Tables 4, 5, 6).

270

### 271 **3.2 Comparison with temperature-based methods**

272 We also compared the performance of the parametric model with two well-known  
273 empirical formulas of Thornthwaite and Blaney-Criddle (Tables 7, 8) by  
274 implementing the same procedure as in the comparison with the radiation-based  
275 methods, i.e. the first 13 years were used as the calibration data set, while the  
276 remaining 7 years were used for validation. Both approaches have wide application in  
277 data-scarce regions. In the CIMIS network the average CE for the Thornthwaite  
278 model was 20.53% for the calibration period and less than zero in the validation  
279 period, while in European stations the CE is 84.58% (calibration) and 78.27%  
280 (validation). The Blaney-Criddle method achieved average CE 69.99% (calibration),  
281 69.82% (validation) in the CIMIS network and 15.69% (calibration) and <0  
282 (validation) in European stations. Finally, the Thornthwaite model seems to be  
283 suitable for use in cold and humid climates (94.84% CE in German stations for the  
284 calibration period) and improper in arid regimes, while for the Blaney-Criddle model  
285 the opposite occurs.

286 **Table 7**

287 **Table 8**

### 288 3.3 Spatial analysis of the parameters

289 The key idea of the parametric model is the replacement of some of the variables and  
290 constants that are used in standardized Penman-Monteith formula by three parameters,  
291 which are regionally varying and estimated through calibration using a reference  
292 evapotranspiration data set. Furthermore, knowledge of the spatial variability of the  
293 PET is crucial in geosciences and the use of the appropriate interpolation technique is  
294 significant (Mancosu *et al.* 2014).

295 In this context, two applications are implemented. The first is the analysis of  
296 the parameters' correlation to latitude and elevation, while the second is their  
297 estimation, through spatial interpolation techniques, along an extensive study area  
298 such as California, which provides sufficient data to perform the necessary calibration  
299 procedures.

300

#### 301 3.3.1 Correlation to latitude and elevation

302 Through regression analysis, we investigated the correlation of every parameter ( $a$ ,  $b$ ,  
303  $c$ ) with latitude  $\varphi$  and elevation. Six scatter plots of Fig. 2, show that parameters  $a$ ,  $b$   
304 are negatively correlated to latitude and elevation, in contrast to parameter  $c$ . This is  
305 similar to the findings of the previous study over the Greek territory (Tegos *et al.*  
306 2013) for parameter  $a$ . There is also noticeable correlation of parameter  $b$  with  
307 elevation ( $R^2 = 0.24$ ) and insignificant correlation of parameter  $c$  with elevation and  
308 latitude. Furthermore, Fig. 2 shows that the relation of the three parameters to latitude  
309 and elevation, according to findings of the present study, appears to be a non-linear  
310 one.

311

312

**Figure 2**

### 313 3.3.2 Spatial interpolation over California

314 Currently, a lot of methods exist which can accomplish spatial interpolation using  
315 available computer codes. In the present study, the three parameters' spatial  
316 variability was investigated by four different methodologies: (1) Inverse Distance  
317 Weighting (IDW); (2) Natural Neighbours (NaN); (3) Ordinary Kriging (OK); and (4)  
318 Bilinear Surface Smoothing (BSS).

319 The first three are well established and commonly used in spatial interpolation  
320 of environmental variables (Li and Heap, 2008). The Bilinear Surface Smoothing  
321 methodology is a new approach that approximates a surface that may be drawn for the  
322 data points with consecutive bilinear surfaces which can be numerically estimated by  
323 means of a least squares fitting procedure into a surface regression model with known  
324 break points and adjustable weights defined by means of angles formed by those  
325 bilinear surfaces. The BSS theory and basic features along with the adjustable  
326 parameters estimation methodology which is based on the generalized cross-  
327 validation methodology are presented in Malamos and Koutsoyiannis (in review) BSS  
328 is implemented by means of a dynamic link library in Object Pascal (Delphi)  
329 programming language linked to Microsoft Excel. The obtained optimal values of the  
330 four adjustable parameters: the number of intervals according to  $x$  and  $y$  directions,  
331 i.e.  $m_x$ ,  $m_y$  and the corresponding smoothing parameters  $\tau_{\lambda_x}$  and  $\tau_{\lambda_y}$ , are presented in  
332 Table 9:

#### 333 **Table 9**

334 IDW and NaN were implemented in ESRI's ArcGIS environment using the  
335 default settings, while for OK all semivariogram models available in that software  
336 were investigated, i.e. circular, exponential, spherical, linear and Gaussian,. In every

337 case, the embedded fitting procedure ensured the minimization of the weighted sum of  
338 squares between experimental and model semivariogram values.

339

340

#### **Table 10**

341 Table 10 presents the values of the statistical criteria for each one of the  
342 implemented semivariogram models, sorted according to the CE criterion for each of  
343 the three parameters. It is obvious that the circular semivariogram achieved the best  
344 overall performance.

345 All three parameters of the parametric model were estimated over California  
346 by applying the four spatial interpolation methods. The input data set consists of the  
347 calculated parameters values at the 39 CIMIS stations (Fig. 3, Table 3).

348

#### **Figure 3**

349

350 Table 11 presents the values of the statistical criteria used to assess the  
351 performance of the spatial interpolation methods with respect to the input data set. It  
352 is apparent that both non-geostatistical methods, according to the statistical criteria  
353 used, outperform ordinary kriging and bilinear surface smoothing, which performed  
354 similarly. This is not a surprise because both IDW and NaN, from construction, are  
355 exact methods of interpolation, so their results respect the data points exactly  
356 (Longley *et al.* 2005, Li and Heap 2008).

357

#### **Table 11**

358 However, the above statistical indices may not be representative with respect  
359 to the validity of the interpolation results in other locations, except for those  
360 incorporated in the interpolation procedure. In this context, a validation procedure was  
361 implemented by means of comparing the reference potential evapotranspiration

362 estimates acquired from the implementation of the parametric method, using the  
363 parameter estimates of the four interpolation methods, against those of the eleven  
364 additional CIMIS stations with adequate time series length, shown in Table 12 along  
365 with the estimated parameter values, in the case of IDW.

366 **Table 12**

367 The performance of each method is presented in Table 13, which summarizes  
368 the CE values acquired from the validation procedure. It is apparent that IDW  
369 outperforms the other three methods in the majority of the cases. This is an interesting  
370 fact, since the IDW method is the effortless of the four methodologies. On the other  
371 hand, the BSS performance is analogous or better to that of the input data set, with CE  
372 values close to those presented in Table 12. NaN and OK performed similarly, with  
373 the first achieving slightly superior outcome, since OK in the case of Borrego Springs  
374 resulted in negative CE value.

375 **Table 13**

376 The variation of the three parameters over California produced by the IDW  
377 technique is illustrated in Fig. 4. It is apparent that both  $a$  and  $c$  present an increasing  
378 North to South gradient, while the opposite occurs for parameter  $b$ . This remark  
379 coincides with the previous findings concerning the relation of the three parameters to  
380 latitude.

381 **Figure 4**

382 **4. Summary and conclusions**

383 The parametric model is a parsimonious radiation-based and physically consistent  
384 approach derived from a simplification of the Penman-Monteith equation, which  
385 requires three parameters to be calibrated prior to its application. By systematic  
386 application of the method the parameters can be eventually provided by maps.



387           The comparison, on the basis of monthly and annual evapotranspiration data,  
388 with commonly used radiation-based models (Hargreaves, McGuinness, Jensen-Haise  
389 and Oudin models) and temperature-based models (Thorthwaite and Blaney-Criddle),  
390 verified the parametric model's high efficiency in different climatic regimes.

391           A parameters analysis, through regression techniques, was conducted in order  
392 to investigate their correlation to latitude and elevation variation. Moreover, the  
393 parameters' spatial estimation was accomplished by implementing interpolation  
394 techniques such as: Inverse Distance Weighting (IDW), Natural Neighbours (NaN),  
395 Ordinary Kriging (OK) and Bilinear Surface Smoothing (BSS), along an extensive  
396 study area such as California. The validation procedure was implemented by  
397 comparing the reference potential evapotranspiration estimates acquired from the  
398 implementation of the parametric method, using the parameter estimates of the four  
399 interpolation methods, against those of the eleven additional CIMIS stations. This  
400 combined evaluation of the four different interpolation approaches, indicated that the  
401 simple and effortless IDW method performs better than the other three methodologies.  
402 Regarding the application of the new methodology, BSS's efficiency to perform  
403 interpolation between data points that are interrelated in a complicated manner was  
404 confirmed, acquiring high CE values analogous to those of the other three methods.

405           Overall, the key idea of the parametric model methodology, which is the  
406 simplification of the Penman-Monteith formula by introducing three parameters,  
407 which are regionally varying and estimated through calibration using a reference  
408 evapotranspiration data set, was very successful.

409           Further research and applications regarding its strengths and weaknesses need  
410 to be conducted in future studies towards: (a) the sensitivity analysis of the three  
411 parameters and therefore the model's performance against the length of the available

412 time series and (b) the implementation of worldwide climatic databases such as the  
413 United Nations Food and Agriculture Organization (UN-FAO) database known as  
414 CLIMWAT (Smith 1993), in order to perform regionalization of the parameters in  
415 world regions with different climatic regimes.

416

#### 417 **Acknowledgements**

418 The authors wish to kindly acknowledge the four anonymous reviewers for their  
419 constructive suggestions which improved earlier versions of this manuscript.

420

#### 421 **References**

- 422 Azhar, A.H., Perera, B.J.C., 2011. Evaluation of Reference Evapotranspiration  
423 Estimation Methods under Southeast Australian Conditions. *J. Irrig. Drain. Eng.*  
424 137, 268–279.
- 425 Alexandris, S., Kerkides, P., 2003. New empirical formula for hourly estimations of  
426 reference evapotranspiration. *Agric. Water Manag.* 60, 157–180.
- 427 Allen, R.G., Jensen, M.E., Wright, J.L., Burman, R.D., 1989. Operational Estimates  
428 of Reference Evapotranspiration. *Agron. J.* 81, 650.
- 429 Blaney, H.F., Criddle, W.D., 1962. Determining consumptive use and irrigation water  
430 requirements (No. 1275). US Department of Agriculture.
- 431 Farquhar, G.D., Roderick M.L., 2007. Worldwide changes in evaporative demand,  
432 Proceedings of the Pontifical Academy of Sciences, 2005.
- 433 Hargreaves, G.H., Samani, Z.A., 1982. Estimating Potential Evapotranspiration. *J.*  
434 *Irrig. Drain. Eng.* 108, 225–230.

435 Hart, Q.J., Brugnach, M., Temesgen, B., Rueda, C., Ustin, S.L., Frame, K., 2009.  
436 Daily reference evapotranspiration for California using satellite imagery and  
437 weather station measurement interpolation. *Civ. Eng. Environ. Syst.* 26, 19–33.

438 Jensen, M.E., Haise, H.R., 1963. Estimating evapotranspiration from solar radiation.  
439 *Proc. Am. Soc. Civ. Eng. J. Irrig. Drain. Div.* 89, 15–41.

440 Klok, E.J., Klein Tank, A.M.G., 2009. Updated and extended European dataset of  
441 daily climate observations. Kozanis, S., Christofides, A., Mamassis, N.,  
442 Efstathiadis, A., Koutsoyiannis D., 2010. Hydrognomon – open source software  
443 for the analysis of hydrological data, EGU General Assembly 2010, Geophysical  
444 Research Abstracts, Vol. 12, Vienna, 12419.

445 Koutsoyiannis, D., Xanthopoulos, Th., 1999. *Engineering Hydrology*, third ed.,  
446 National Technical University of Athens, Athens.  
447 (<http://www.itia.ntua.gr/en/docinfo/115/>)

448 Koutsoyiannis, D., 2009. Seeking parsimony in hydrology and water resources  
449 technology (solicited), European Geosciences Union General Assembly 2009,  
450 *Geophysical Research Abstracts*, Vol. 11, Vienna, 11469.  
451 (<http://www.itia.ntua.gr/en/docinfo/906/>)

452 Koutsoyiannis, D., 2014. Reconciling hydrology with engineering. *Hydrol. Res.* 45  
453 (1), 2-24.

454 Li, J., Heap, A.D., 2008. *A Review of Spatial Interpolation Methods for*  
455 *Environmental Scientists*, Geoscience Australia. Geoscience Australia, GPO Box  
456 378, Canberra, ACT 2601, Australia.

457 Longley, P.A., Goodchild, M.F., Maguire, D.J., Rhind, D.W., 2005. *Geographic*  
458 *information system and Science*, second ed, England: John Wiley & Sons, Ltd,  
459 West Sussex PO19 8SQ, England, pp. 333–335.

460 Lu, J., Sun, G., McNulty, S.G., Amatya, D.M., 2005. A comparison of six potential  
461 comparison evapotranspiration methods for regional use in the Southeastern  
462 United States. *J. Am. Water Resour. Assoc.* 41, 621–633.

463 Malamos, N. and Koutsoyiannis, D., in review. Bilinear surface smoothing for spatial  
464 interpolation with optional incorporation of an explanatory variable. Part 1:  
465 Theory, *Hydrol. Sci. J.*

466 Mamassis, N., Panagoulia, D., Novcovic, A., 2014. Sensitivity analysis of Penman  
467 evaporation method, *Global NEST Journal*, Vol.16, No 4, pp. 628-639.

468 Mancosu, N., Snyder, R.L., Spano, D., 2014. Procedures to Develop a Standardized  
469 Reference Evapotranspiration Zone Map. *J. Irrig. Drain. Eng.* 140, A4014004.

470 McGuinness J.L, Bordne E.F, 1972. A comparison of lysimeter- derived potential  
471 evapotranspiration with computed values, Technical Bulletin 1452, Agricultural  
472 Research Service, US Department of Agriculture, Washington, DC

473 McMahon, T.A., Peel, M.C., Lowe, L., Srikanthan, R., McVicar, T.R., 2013.  
474 Estimating actual, potential, reference crop and pan evaporation using standard  
475 meteorological data: a pragmatic synthesis. *Hydrol. Earth Syst. Sci.* 17, 1331–  
476 1363.

477 Monteith, J.L., 1981. Evaporation and environment. *Symp. Soc. Exp. Biol.* Vol. 19.  
478 No. 205-23.

479 Monteith, J.L., 1981. Evaporation and surface temperature. *Q. J. R. Meteorol. Soc.*  
480 107, 1–27.

481 Moriasi, D.N., Arnold, J.G., Van Liew, M.W., Bingner, R.L., Harmel, R.D., Veith,  
482 T.L., 2007. Model Evaluation Guidelines for Systematic Quantification of  
483 Accuracy in Watershed Simulations. *Trans. ASABE* 50, 885–900.

484 Nash, J.E., Sutcliffe, J.V., 1970. River flow forecasting through conceptual models  
485 part I - A discussion of principles. *J. Hydrol.* 10, 282–290.

486 Irmak, S., Allen, R.G., Whitty, E.B., 2003. Daily Grass and Alfalfa-Reference  
487 Evapotranspiration Estimates and Alfalfa-to-Grass Evapotranspiration Ratios in  
488 Florida. *J. Irrig. Drain. Eng.* 129, 360–370.

489 Pereira, A.R., Pruitt, W.O., 2004. Adaptation of the Thornthwaite scheme for  
490 estimating daily reference evapotranspiration. *Agric. Water Manag.* 66, 251–257.

491 Oudin, L., Hervieu, F., Michel, C., Perrin, C., Andréassian, V., Anctil, F., Loumagne,  
492 C., 2005. Which potential evapotranspiration input for a lumped rainfall–runoff  
493 model?: Part 2-Towards a simple and efficient potential evapotranspiration  
494 model for rainfall–runoff modelling. *J. Hydrol.* 303, 290–306.

495 Samani, Z., 2000. Estimating Solar Radiation and Evapotranspiration Using  
496 Minimum Climatological Data. *J. Irrig. Drain. Eng.* 126, 265–267.

497 Samaras, D.A., Reif, A., Theodoropoulos, K., 2013. Evaluation of Radiation-Based  
498 Reference Evapotranspiration Models Under Different Mediterranean Climates  
499 in Central Greece. *Water Resour. Manag.* 28, 207–225.

500 Shahidian, S., Serralheiro, R.P., Serrano, J., Teixeira, J.L., 2013. Parametric  
501 calibration of the Hargreaves-Samani equation for use at new locations. *Hydrol.*  
502 *Process.* 27, 605–616.

503 Smith, M., 1993. CLIMWAT for CROPWAT: A climatic database for irrigation  
504 planning and management. FAO Irrigation and Drainage Paper No. 49, Rome.  
505 (CLIMWAT 2.0), [http://www.fao.org/nr/water/infores\\_databases\\_climwat.html](http://www.fao.org/nr/water/infores_databases_climwat.html).

506 Tabari, H., 2009. Evaluation of Reference Crop Evapotranspiration Equations in  
507 Various Climates. *Water Resour. Manag.* 24, 2311–2337.

508 Tabari, H., Talaei, P.H., 2011. Local Calibration of the Hargreaves and Priestley-  
509 Taylor Equations for Estimating Reference Evapotranspiration in Arid and Cold  
510 Climates of Iran Based on the Penman-Monteith Model. *J. Hydrol. Eng.* 16, 837–  
511 845.

512 Tegos A., Efstratiadis A., Koutsoyiannis D., 2013. A Parametric Model for Potential  
513 Evapotranspiration Estimation Based on a Simplified Formulation of the  
514 Penman- Monteith Equation. In: *Evapotranspiration-An Overview*. S.  
515 Alexandris.(Ed.), InTech, pp. 143-165.  
516 (<http://www.itia.ntua.gr/en/docinfo/1284/>)

517 Tegos, A., Mamassis, N., Koutsoyiannis, D., 2009. Estimation of potential  
518 evapotranspiration with minimal data dependence. *EGU General Assembly*  
519 *Conference Abstracts*. Vol. 11. (<http://www.itia.ntua.gr/en/docinfo/905/>)

520 Thepadia, M., Martinez, C.J., 2012. Regional Calibration of Solar Radiation and  
521 Reference Evapotranspiration Estimates with Minimal Data in Florida. *J. Irrig.*  
522 *Drain. Eng.* 138, 111–119.

523 Thornthwaite, C.W., 1948. An approach toward a rational classification of  
524 climate. *Geographical Review*, 55-94.

525 Xu, C.Y., Singh, V.P., 2001. Evaluation and generalization of temperature-based  
526 methods for calculating evaporation. *Hydrol. Process.* 15, 305–319.

527 Xu, C.Y., Singh, V.P., 2002. Cross comparison of empirical equations for calculating  
528 potential evapotranspiration with data from Switzerland. *Water Resour. Manag.*  
529 16, 197–219.

530 Wang, J., Georgakakos, K.P., 2007. Estimation of potential evapotranspiration in the  
531 mountainous Panama Canal watershed. *Hydrol. Process.* 21, 1901–1917.

532 Valiantzas, J.D., 2013. Simplified forms for the standardized FAO-56 Penman–  
533 Monteith reference evapotranspiration using limited weather data. *J. Hydrol.*  
534 505, 13–23.

**Table 1** Radiation-based methods for potential evapotranspiration estimation

Method	Jensen and Haise	Mcguinness and Bordne	Hargreaves	Oudin
PET expression	$\frac{R_a T_a}{40 \lambda \rho}$	$\frac{R_a (T_a + 5)}{68 \lambda \rho}$	$0.0023 \frac{R_a}{\lambda} (T_a + 17.8) (T_{\max} - T_{\min})^{0.5}$	$\frac{R_a (T_a + 5)}{100 \lambda \rho}$

**Table 2** Meteorological stations used for the evaluation of the potential evapotranspiration methods

No.	Station name, Location	No.	Station name, Location	No.	Station name, Location
1	Five Points, U.S.A.	19	Buntigville, U.S.A.	37	De Laveaga, U.S.A.
2	Davis, U.S.A.	20	Temecula, U.S.A.	38	Westlands, U.S.A.
3	Firebaugh Teles, U.S.A.	21	Santa Ynez, U.S.A.	39	Sanel Valley, U.S.A.
4	Gerber, U.S.A.	22	Seeley, U.S.A.	40	Aachen, Germany
5	Durham, U.S.A.	23	Manteca, U.S.A.	41	Angermunde, Germany
6	Carmino, U.S.A.	24	Modesto, U.S.A.	42	Bremen-Seefahrtshule, Germany
7	Stratford, U.S.A.	25	Irvine, U.S.A.	43	Dresden-Klotzsche, Germany
8	Castorville, U.S.A.	26	Oakville, U.S.A.	44	Dusseldorf, Germany
9	Kettleman, U.S.A.	27	Pomona, U.S.A.	45	Frankfurt, Germany
10	Bishop, U.S.A.	28	Frenso State, U.S.A.	46	Hamburg Fuhlsbuettel, Germany
11	Parlier, U.S.A.	29	Santa Rosa, U.S.A.	47	Karlsruhue, Germany
12	Calipatria, U.S.A.	30	Browns Valley, U.S.A.	48	Muenchen-Flughafen, Germany
13	Mc Arthur, U.S.A.	31	Lindcove, U.S.A.	49	Stuggart-Schnarreberg, Germany
14	UC Riverside, U.S.A.	32	Meloland, U.S.A.	50	Alicante, Spain
15	Brentwood, U.S.A.	33	Alturas, U.S.A.	51	Badajoz Televera, Spain
16	San Luis Obispo, U.S.A.	34	Cuyama, U.S.A.	52	Valencia, Spain
17	Blackwells Corner, U.S.A.	35	Tulelake, U.S.A.	53	Zaragoza Aeropuerto, Spain
18	Los Banos, U.S.A.	36	Windsor, U.S.A.		

**Table 3** Meteorological stations numbers and corresponding parameter values for the parametric method

Station No.	$a$ (kg kJ <sup>-1</sup> )	$b$ (kg m <sup>-2</sup> )	$c$ (°C <sup>-1</sup> )	Station No.	$a$ (kg kJ <sup>-1</sup> )	$b$ (kg m <sup>-2</sup> )	$c$ (°C <sup>-1</sup> )
1	1.47 10 <sup>-4</sup>	1.49	1.58 10 <sup>-2</sup>	28	1.29 10 <sup>-4</sup>	1.3	1.73 10 <sup>-2</sup>
2	1.04 10 <sup>-4</sup>	6.51 10 <sup>-1</sup>	2.15 10 <sup>-2</sup>	29	8.88 10 <sup>-5</sup>	6.09 10 <sup>-1</sup>	2.63 10 <sup>-2</sup>



3	1.46 10 <sup>-4</sup>	1.48	1.47 10 <sup>-2</sup>	30	8.95 10 <sup>-5</sup>	4.07 10 <sup>-1</sup>	2.11 10 <sup>-2</sup>
4	1.02 10 <sup>-4</sup>	4.97 10 <sup>-1</sup>	1.93 10 <sup>-2</sup>	31	1.12 10 <sup>-4</sup>	1.04	1.74 10 <sup>-2</sup>
5	1.97 10 <sup>-4</sup>	2.07	-2.70 10 <sup>-4</sup>	32	2.12 10 <sup>-4</sup>	2	4.94 10 <sup>-3</sup>
6	8.82 10 <sup>-5</sup>	2.49 10 <sup>-1</sup>	2.34 10 <sup>-2</sup>	33	7.92 10 <sup>-5</sup>	-2.20 10 <sup>-1</sup>	2.44 10 <sup>-2</sup>
7	1.12 10 <sup>-4</sup>	-2.50 10 <sup>-1</sup>	1.44 10 <sup>-2</sup>	34	1.08 10 <sup>-4</sup>	4.03 10 <sup>-1</sup>	1.97 10 <sup>-2</sup>
8	1.68 10 <sup>-4</sup>	1.06	-3.60 10 <sup>-2</sup>	35	9.28 10 <sup>-5</sup>	5.20 10 <sup>-2</sup>	2.12 10 <sup>-2</sup>
9	1.34 10 <sup>-4</sup>	1.23	1.62 10 <sup>-2</sup>	36	8.65 10 <sup>-5</sup>	5.66 10 <sup>-1</sup>	2.60 10 <sup>-2</sup>
10	1.43 10 <sup>-4</sup>	7.39 10 <sup>-1</sup>	1.05 10 <sup>-2</sup>	37	1.02 10 <sup>-4</sup>	5.82 10 <sup>-1</sup>	1.24 10 <sup>-2</sup>
11	1.29 10 <sup>-4</sup>	1.32	1.61 10 <sup>-2</sup>	38	1.40 10 <sup>-4</sup>	1.33	1.67 10 <sup>-2</sup>
12	1.69 10 <sup>-4</sup>	1.32	8.86 10 <sup>-3</sup>	39	9.88 10 <sup>-5</sup>	6.54 10 <sup>-1</sup>	2.37 10 <sup>-2</sup>
13	9.75 10 <sup>-5</sup>	4.26 10 <sup>-1</sup>	2.36 10 <sup>-2</sup>	40	3.96 10 <sup>-5</sup>	-2.46 10 <sup>-1</sup>	2.62 10 <sup>-2</sup>
14	8.68 10 <sup>-5</sup>	5.10 10 <sup>-2</sup>	1.78 10 <sup>-2</sup>	41	3.96 10 <sup>-5</sup>	-2.58 10 <sup>-1</sup>	2.73 10 <sup>-2</sup>
15	1.11 10 <sup>-4</sup>	9.00 10 <sup>-1</sup>	2.09 10 <sup>-2</sup>	42	4.28 10 <sup>-5</sup>	-1.64 10 <sup>-1</sup>	2.68 10 <sup>-2</sup>
16	8.10 10 <sup>-5</sup>	1.60 10 <sup>-1</sup>	2.28 10 <sup>-2</sup>	43	3.67 10 <sup>-5</sup>	-3.45 10 <sup>-1</sup>	2.81 10 <sup>-2</sup>
17	1.21 10 <sup>-4</sup>	1.02	1.89 10 <sup>-2</sup>	44	4.12 10 <sup>-5</sup>	-3.02 10 <sup>-1</sup>	2.64 10 <sup>-2</sup>
18	1.31 10 <sup>-4</sup>	1.31	1.81 10 <sup>-2</sup>	45	4.75 10 <sup>-5</sup>	-8.8 10 <sup>-2</sup>	2.62 10 <sup>-2</sup>
19	9.29 10 <sup>-5</sup>	-1.10 10 <sup>-1</sup>	2.11 10 <sup>-2</sup>	46	4.18 10 <sup>-5</sup>	-1.66 10 <sup>-1</sup>	2.66 10 <sup>-2</sup>
20	6.66 10 <sup>-5</sup>	-2.80 10 <sup>-1</sup>	2.10 10 <sup>-2</sup>	47	4.64 10 <sup>-5</sup>	-6.6 10 <sup>-2</sup>	2.58 10 <sup>-2</sup>
21	9.44 10 <sup>-5</sup>	4.91 10 <sup>-1</sup>	2.06 10 <sup>-2</sup>	48	4.69 10 <sup>-5</sup>	-8.8 10 <sup>-2</sup>	2.51 10 <sup>-2</sup>
22	2.50 10 <sup>-4</sup>	2.58	7.52 10 <sup>-4</sup>	49	4.53 10 <sup>-5</sup>	-1.64 10 <sup>-1</sup>	2.52 10 <sup>-2</sup>
23	1.13 10 <sup>-4</sup>	1.02	2.03 10 <sup>-2</sup>	50	5.89 10 <sup>-5</sup>	-4.67 10 <sup>-1</sup>	1.84 10 <sup>-2</sup>
24	1.17 10 <sup>-4</sup>	1.08	2.00 10 <sup>-2</sup>	51	6.24 10 <sup>-5</sup>	1.72 10 <sup>-1</sup>	2.35 10 <sup>-2</sup>
25	6.64 10 <sup>-5</sup>	-4.40 10 <sup>-2</sup>	2.28 10 <sup>-2</sup>	52	5.34 10 <sup>-5</sup>	-1.93 10 <sup>-1</sup>	1.96 10 <sup>-2</sup>
26	8.42 10 <sup>-5</sup>	4.29 10 <sup>-1</sup>	2.54 10 <sup>-2</sup>	53	7.00 10 <sup>-5</sup>	-2.2 10 <sup>-2</sup>	2.39 10 <sup>-2</sup>
27	1.13 10 <sup>-4</sup>	1.25	2.00 10 <sup>-2</sup>				

**Table 4** Values of performance indices used to evaluate the parametric method, in the estimation of mean annual potential evapotranspiration for the 39 CIMIS stations, against the other four models

Method	CE (%)	MBE (mm)	MAE (mm)	RMSE (mm)
Parametric	99.1	4	6	17
Hargreaves	78.9	2	60	82
Jensen-Haise	< 0	417	452	493
McGuinness	30.1	19	111	149
Oudin	< 0	-393	393	411

**Table 5** Distribution of CE values of radiation-based approaches in CIMIS network

CE (%)	Parametric	Hargreaves	Jensen-Haise	McGuinness	Oudin

	Cal	Val	Cal	Val	Cal	Val	Cal	Val	Cal	Val
95-100	26	26	26	23	0	7	16	15	0	0
90-95	11	5	10	7	0	2	6	7	0	0
80-90	2	8	3	9	1	2	10	10	1	0
70-80	0	0	0	0	6	3	3	3	3	5
60-70	0	0	0	0	1	6	2	3	7	4
50-60	0	0	0	0	3	4	1	1	12	6
0-50	0	0	0	0	16	9	1	0	16	24
<0	0	0	0	0	12	6	0	0	0	0

**Table 6** Distribution of CE values of radiation-based approaches in European stations

CE	Parametric		Hargreaves		Jensen-Haise		Mcguinness		Oudin	
	Cal	Val	Cal	Val	Cal	Val	Cal	Val	Cal	Val
95-100	10	9	6	0	0	0	0	0	9	1
90-95	4	4	4	6	0	0	0	0	2	8
80-90	0	0	3	7	0	0	0	0	0	2
70-80	0	0	1	1	0	0	7	1	1	1
60-70	0	0	0	0	0	0	3	1	1	1
50-60	0	0	0	0	0	0	3	1	1	0
0-50	0	1	0	0	5	1	2	9	0	1
<0	0	0	0	0	9	13	1	2	0	0

**Table 7** Distribution of CE values of temperature-based approaches in CIMIS network

CE	Thornthwaite		Blaney-Criddle	
	Cal	Val	Cal	Val
95-100	0	0	0	0
90-95	0	0	0	0
80-90	0	0	10	16
70-80	0	0	18	12
60-70	1	0	5	5
50-60	4	3	2	1
0-50	24	21	3	4
<0	10	15	1	1

**Table 8** Distribution of CE values of temperature-based approaches in European stations

CE	Thornthwaite		Blaney-Criddle	
	Cal	Val	Cal	Val
95-100	5	0	0	0

90-95	5	1	0	0
80-90	0	9	0	0
70-80	2	1	1	1
60-70	0	1	0	0
50-60	1	1	0	1
0-50	1	1	12	1
<0	0	0	1	11

**Table 9** BSS parameters optimal values, for the California application

Parameter	mx	my	$\tau_{\lambda x}$	$\tau_{\lambda y}$
$a$ (kg kJ <sup>-1</sup> )	3	8	0.082	0.001
$b$ (kg m <sup>-2</sup> )	3	28	0.001	0.01
$c$ (°C <sup>-1</sup> )	3	8	0.001	0.001

**Table 10** Values of the statistical criteria used to assess the performance of the different kriging semivariogram models

Parameter	kriging semivariogram	CE (%)	MBE	MAE	RMSE
$a$ (kg kJ <sup>-1</sup> )	circular	99.9	1.03 10 <sup>-8</sup>	5.18 10 <sup>-7</sup>	8.93 10 <sup>-7</sup>
	exponential	99.9	1.03 10 <sup>-8</sup>	5.18 10 <sup>-7</sup>	8.93 10 <sup>-7</sup>
	spherical	99.9	1.03 10 <sup>-8</sup>	5.18 10 <sup>-7</sup>	8.93 10 <sup>-7</sup>
	linear	99.9	1.03 10 <sup>-8</sup>	5.18 10 <sup>-7</sup>	8.93 10 <sup>-7</sup>
	gaussian	44.6	1.24 10 <sup>-6</sup>	1.86 10 <sup>-5</sup>	2.88 10 <sup>-5</sup>
$b$ (kg m <sup>-2</sup> )	circular	68.6	4.24 10 <sup>-3</sup>	2.71 10 <sup>-1</sup>	3.68 10 <sup>-1</sup>
	exponential	72.8	3.12 10 <sup>-3</sup>	2.50 10 <sup>-1</sup>	3.43 10 <sup>-1</sup>
	spherical	67.4	5.46 10 <sup>-3</sup>	2.77 10 <sup>-1</sup>	3.76 10 <sup>-1</sup>
	linear	66.6	6.00 10 <sup>-3</sup>	2.81 10 <sup>-1</sup>	3.80 10 <sup>-1</sup>
	gaussian	29.7	4.09 10 <sup>-2</sup>	4.07 10 <sup>-1</sup>	5.51 10 <sup>-1</sup>
$c$ (°C <sup>-1</sup> )	circular	39.3	3.56 10 <sup>-4</sup>	4.62 10 <sup>-3</sup>	8.19 10 <sup>-3</sup>
	exponential	11.0	4.67 10 <sup>-4</sup>	5.62 10 <sup>-3</sup>	9.92 10 <sup>-3</sup>
	spherical	11.7	4.64 10 <sup>-4</sup>	5.60 10 <sup>-3</sup>	9.88 10 <sup>-3</sup>
	linear	11.0	4.67 10 <sup>-4</sup>	5.62 10 <sup>-3</sup>	9.92 10 <sup>-3</sup>
	gaussian	11.0	4.67 10 <sup>-4</sup>	5.62 10 <sup>-3</sup>	9.92 10 <sup>-3</sup>

**Table 11** Values of the statistical criteria used to assess the performance of the spatial interpolation methods with respect to the input data set

Parameter	Interpolation Method	CE (%)	MBE	MAE	RMSE
$a$ (kg kJ <sup>-1</sup> )	IDW	100	$3.59 \cdot 10^{-8}$	$1.08 \cdot 10^{-7}$	$1.97 \cdot 10^{-7}$
	NaN	100	$-1.03 \cdot 10^{-7}$	$4.77 \cdot 10^{-7}$	$8.95 \cdot 10^{-7}$
	OK	99.9	$1.03 \cdot 10^{-8}$	$5.18 \cdot 10^{-7}$	$8.93 \cdot 10^{-7}$
	BSS	73.2	$4.36 \cdot 10^{-8}$	$1.35 \cdot 10^{-5}$	$2.01 \cdot 10^{-5}$
$b$ (kg m <sup>-2</sup> )	IDW	100	$2.95 \cdot 10^{-4}$	$1.72 \cdot 10^{-3}$	$3.06 \cdot 10^{-3}$
	NaN	99.9	$-9.48 \cdot 10^{-4}$	$1.16 \cdot 10^{-2}$	$2.12 \cdot 10^{-2}$
	OK	68.6	$4.24 \cdot 10^{-3}$	$2.71 \cdot 10^{-1}$	$3.68 \cdot 10^{-1}$
	BSS	65.2	$1.97 \cdot 10^{-4}$	$2.68 \cdot 10^{-1}$	$3.88 \cdot 10^{-1}$
$c$ (°C <sup>-1</sup> )	IDW	100	$2.56 \cdot 10^{-7}$	$8.82 \cdot 10^{-6}$	$1.52 \cdot 10^{-5}$
	NaN	99.9	$1.54 \cdot 10^{-6}$	$1.50 \cdot 10^{-4}$	$3.10 \cdot 10^{-4}$
	OK	39.3	$3.56 \cdot 10^{-4}$	$4.62 \cdot 10^{-3}$	$8.19 \cdot 10^{-3}$
	BSS	68.9	$-2.57 \cdot 10^{-7}$	$3.25 \cdot 10^{-3}$	$5.87 \cdot 10^{-3}$

**Table 12** CIMIS Stations used for validation purposes and estimated parameters values in the case of IDW

Station	$a$ (kg kJ <sup>-1</sup> )	$b$ (kg m <sup>-2</sup> )	$c$ (°C <sup>-1</sup> )
Arroyo Seco	$1.38 \cdot 10^{-4}$	1.06	$1.20 \cdot 10^{-3}$
Carneros	$9.10 \cdot 10^{-5}$	$5.48 \cdot 10^{-1}$	$2.42 \cdot 10^{-2}$
Green Valey Road	$1.16 \cdot 10^{-4}$	$7.75 \cdot 10^{-1}$	$7.26 \cdot 10^{-3}$
King City Oasis	$1.34 \cdot 10^{-4}$	1.09	$9.53 \cdot 10^{-3}$
Santa Barbara	$1.03 \cdot 10^{-4}$	$5.56 \cdot 10^{-1}$	$1.98 \cdot 10^{-2}$
Alpaugh	$1.23 \cdot 10^{-4}$	$8.27 \cdot 10^{-1}$	$1.67 \cdot 10^{-2}$
Auburn	$1.04 \cdot 10^{-4}$	$6.20 \cdot 10^{-1}$	$1.99 \cdot 10^{-2}$
Borrego Springs	$1.73 \cdot 10^{-4}$	1.44	$9.33 \cdot 10^{-3}$
Lodi West	$1.10 \cdot 10^{-4}$	$8.54 \cdot 10^{-1}$	$2.05 \cdot 10^{-2}$
Merced	$1.30 \cdot 10^{-4}$	1.20	$1.73 \cdot 10^{-2}$
Palmdale	$1.01 \cdot 10^{-4}$	$7.86 \cdot 10^{-1}$	$2.00 \cdot 10^{-2}$

**Table 13** CE values for every interpolation method in validation procedure stations

Station	IDW	NaN	OK	BSS
Arroyo Seco	77.7	78.9*	76.8	66.8
Carneros	96.1	96.2*	83.6	95.9
Green Valey Road	71.6*	69.5	70.2	65.7
King City Oasis	85.1	60.3	93.6*	64.3
Santa Barbara	47.9	72.4	78.2*	23.4
Alpaugh	95.7	95.5	96.0*	95.9
Auburn	94.4*	93.6	94.3	85.8
Borrego Springs	85.3*	81.3	<0	70.1
Lodi West	94.0*	93.7	92.9	92.3
Merced	96.9	97.1*	96.9	89.5
Palmdale	69.6	70.3	91.1*	56.0

\* denotes each station's highest CE value

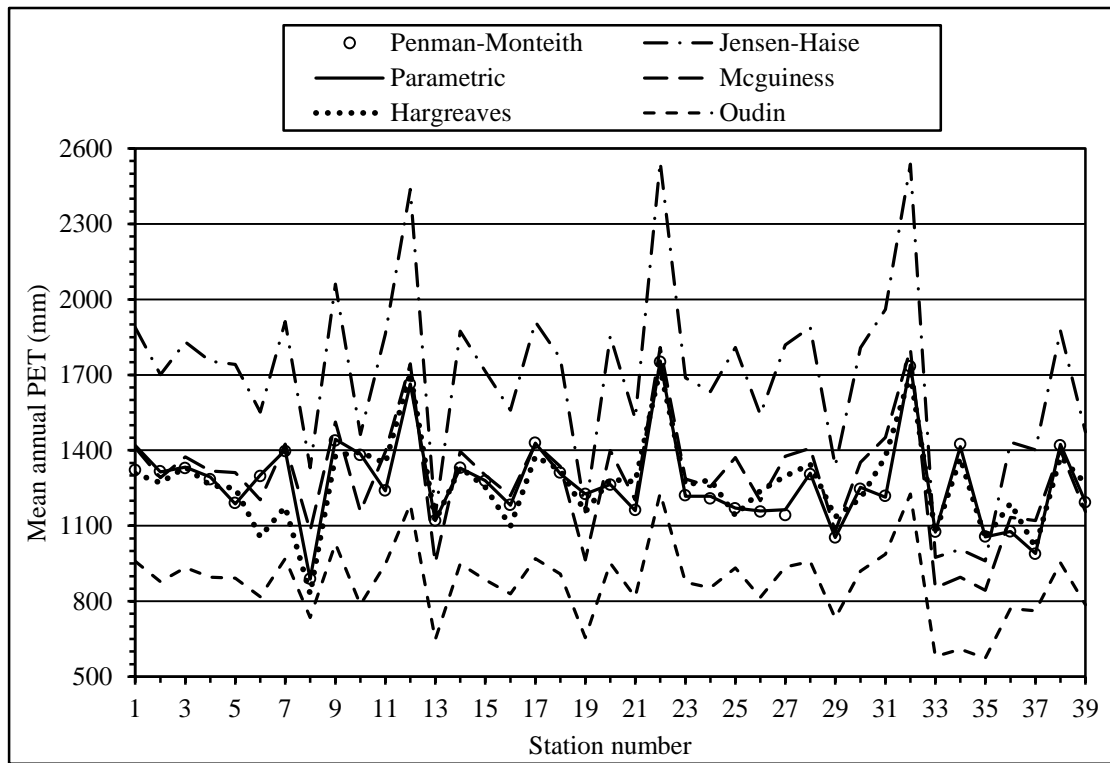


**Fig. 1** Mean annual Penman-Monteith potential evapotranspiration (symbols) for the 39 CIMIS stations against the parametric model and the other four methods

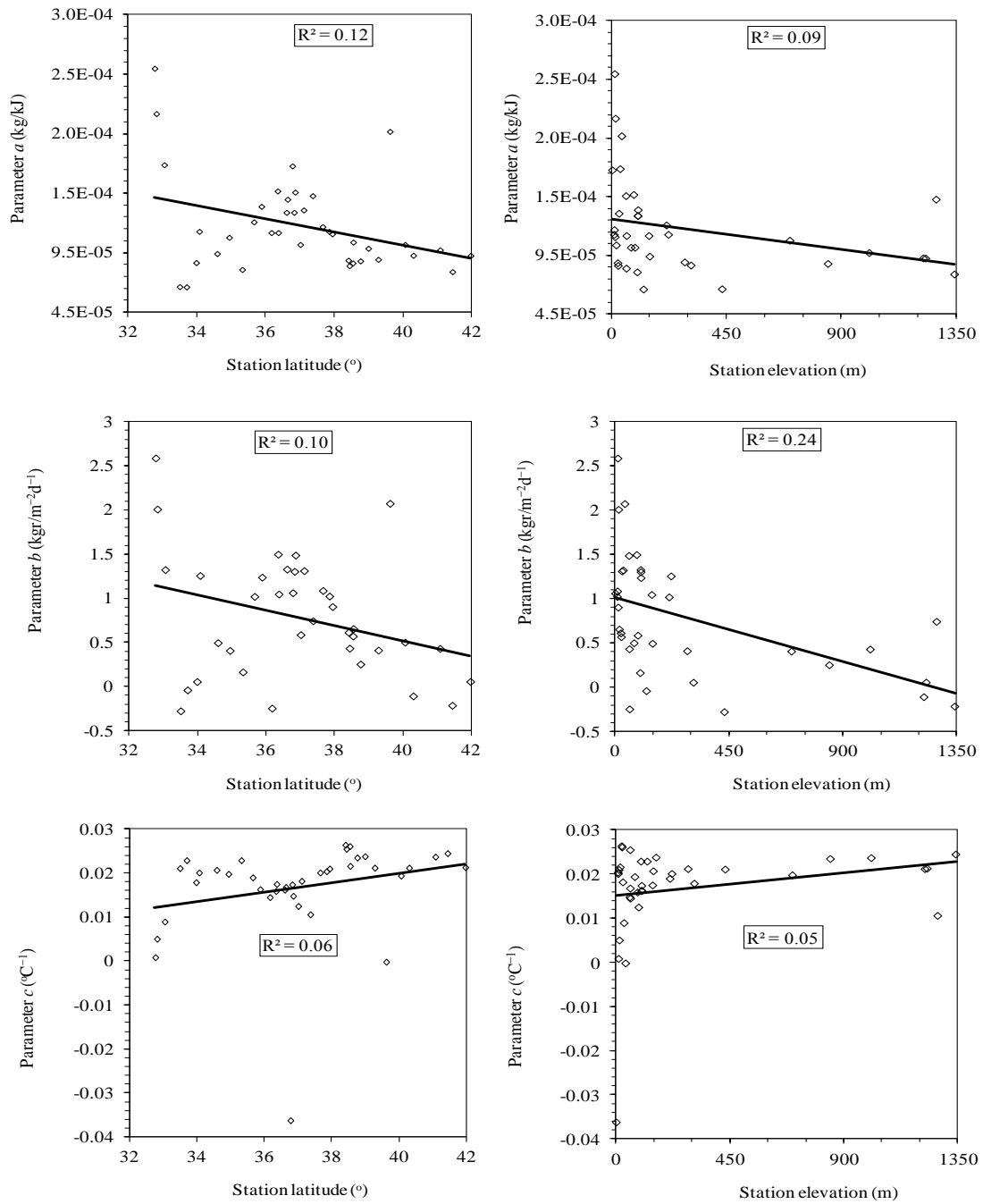


**Fig. 2** Scatter plots of parameters against latitude and elevation

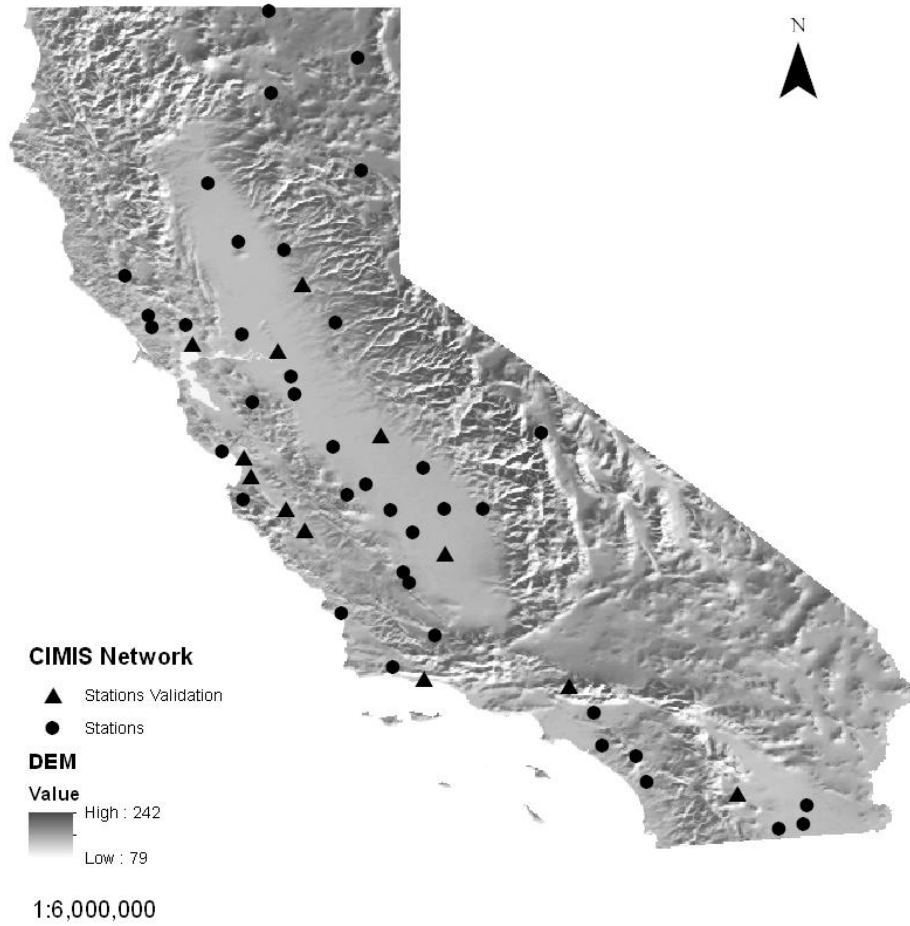


**Fig. 3** Study area and the CIMIS Stations used for spatial analysis



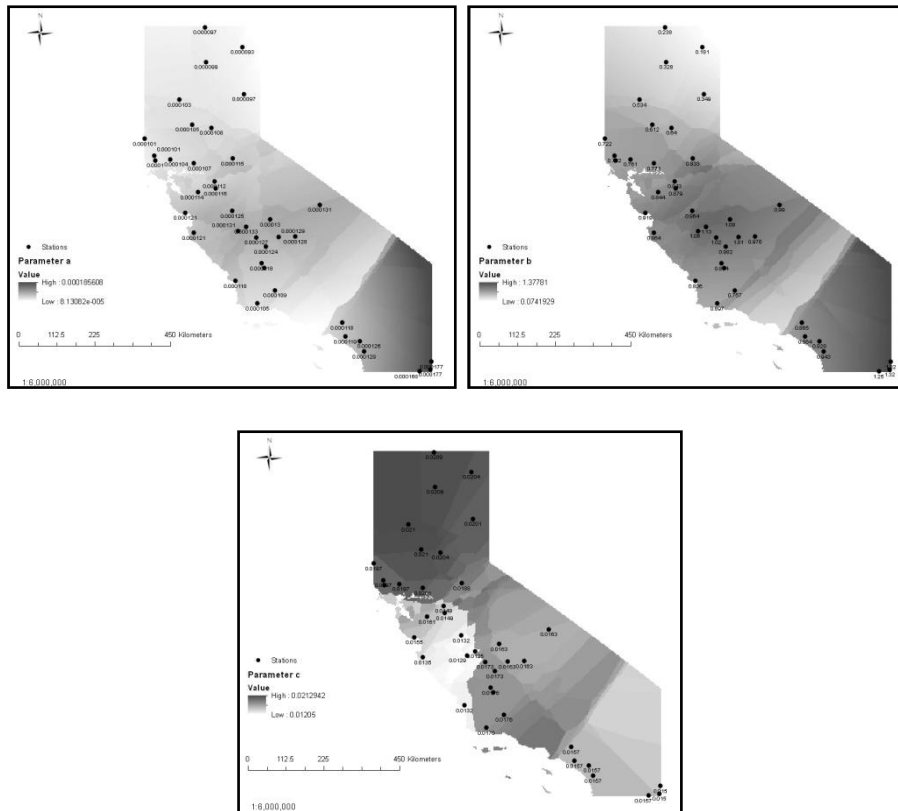


**Fig. 4** Parameters maps produced by the IDW method, for the California region